R. GATI[✉]
M. ALBIEZ
J. FÖLLING
B. HEMMERLING
M.K. OBERTHALER

Realization of a single Josephson junction for Bose–Einstein condensates

Kirchhoff Institut für Physik, University of Heidelberg, Im Neuenheimer Feld 227, 69120 Heidelberg, Germany

ABSTRACT We report on the realization of a double-well potential for Rubidium-87 Bose-Einstein condensates. The experimental setup allows for the investigation of two different dynamical phenomena known for this system – Josephson oscillations and self-trapping. We give a detailed discussion of the experimental setup and the methods used for calibrating the relevant parameters. We compare our experimental findings with the predictions of an extended two-mode model and find quantitative agreement.

PACS 74.50.+r; 03.75.Lm; 05.45.-a

1   Introduction

One of the most prominent features of quantum mechanics is the tunnelling of massive particles through classically forbidden regions. Although tunnelling is a purely quantum mechanical effect, it can be observed on a macroscopic scale if the system can be described by two weakly linked (i.e. having a small spatial overlap) macroscopic wave functions with global phase coherence. A fundamental physical phenomenon based on macroscopic tunnelling is the Josephson effect predicted by Brian D. Josephson in 1962 [1]. The first observation of this effect has been realized with two superconductors separated by a thin insulating barrier and was reported by Anderson et al. [2] just one year after its theoretical prediction. Since then many experiments with the electronic Josephson junction system have been performed. The Josephson effect has also found its way to technological applications such as superconducting quantum interference devices (SQUIDS) which allow measurement of weak magnetic fields with very high precision.

The Josephson effect for neutral superfluids has already been observed with liquid ^{3}He [3] and ^{4}He [4] exhibiting the typical current-phase relation. It is characterized by an alternating current flowing through the central tunnelling barrier if a constant energy difference between both sides is applied. In the context of dilute quantum gases such as Bose–Einstein condensates (BECs) Josephson junction arrays have

✉ Fax: +49 6221 549869, E-mail: bec@matterwave.de

been demonstrated [5] and only recently a single weak link was realized, and the predicted tunnelling dynamics have been observed [6]. The main subject of this paper is the discussion of this experimental setup. We will give a detailed description of the experimental implementation and the necessary thorough calibration of the system parameters. We are also going to discuss the comparison of the obtained data with an improved two-mode model recently developed by D. Ananikian and T. Bergeman [7].

2   Basic setup

There are many different methods to produce a double-well potential for Bose–Einstein condensates. The first realized double-well potential was obtained already in the early days of BEC using a harmonic confinement created by a magnetic trap and a focussed blue detuned laser beam generating the tunnelling barrier. This setup with a well separation of typically 50 μm was used for the first interference measurements with BECs [8]. Many other attempts have been made to realize double-well potentials [9–11] but so far only the splitting of condensates into two independent parts was possible. Recently we succeeded in observing Josephson dynamics in a double-well potential realized with optical dipole potentials [6]. The basic idea is the combination of a three dimensional harmonic confinement and a one dimensional periodic potential with a large lattice spacing of 5 μm (see Fig. 1).

The ^{87}Rb BEC in our experiment is prepared in a crossed beam dipole trap consisting of two orthogonal far red detuned Nd-Yag laser beams (see Fig. 1). A frequency difference of 10 MHz between the two beams is introduced in order to avoid uncontrolled interferences between both beams. The dipole trap beam is radially symmetric and has a waist of 60 (5) μm. It provides confinement in the direction of gravity (in the following discussion the z-direction) and in the y-direction. The crossed dipole beam is radially asymmetric and has a radius at the intersection of 140 (5) μm in the z-direction and 70 (5) μm in the x-direction. This asymmetry allows the adjustment of the harmonic confinement along the x-direction, i.e. the direction of the double-well potential, without significantly changing the trap frequencies in the other directions. With a maximum power of approximately 500 mW in the dipole trap beam and 800 mW in the crossed dipole beam,
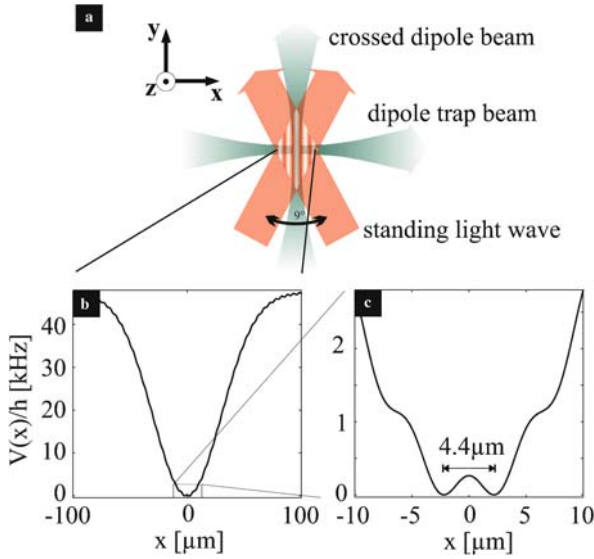
FIGURE 1 Realization of a single Josephson junction using optical dipole potentials. (**a**) The basic setup is given by a crossed beam dipole trap combined with a periodic light shift potential implemented with two beams intersecting under an angle of 9°. (**b**) On the scale of the three dimensional harmonic confinement the periodic potential is hardly visible. (**c**) In the center of the combined potential a clean double-well potential is realized

we can achieve a maximum three-dimensional confinement of $\omega_{x,\max} \approx 2\pi \times 120\,(6)$ Hz, $\omega_{y,\max} \approx 2\pi \times 170\,(8)$ Hz and $\omega_{z,\max} \approx 2\pi \times 180\,(8)$ Hz, and a maximum trap depth of approximately 5 μK. The typical spontaneous emission rate is estimated to be 0.01 Hz and thus is negligible for all our experiments.

The periodic potential is realized by a pair of laser beams with parallel linear polarization crossing at a relative angle of $\alpha = 9(1)°$ as depicted in Fig. 1a. The beams are aligned symmetrically with respect to the crossed dipole beam, such that the resulting potential is modulated only in the x-direction. The laser wavelength is chosen to be 811 nm. The resulting potential is shown in Fig. 1b,c and is given by

$$V_{\mathrm{d}w} = \frac{1}{2}mw_x^2(x - \Delta x)^2 + V_0 \cos^2\left(\frac{\pi x}{d_\mathrm{l}}\right), \qquad (1)$$

where Δx is the relative position of the two potentials. For $\Delta x = 0$ a symmetric double-well potential is obtained.

The intensities of all laser beams and the relative distance between the center of the crossed dipole beam and a maximum of the periodic potential are very critical parameters thus an active stabilization is inevitable. The light intensities are stabilized to better than 10^{-4} which allows the generation of small condensates with small shot-to-shot fluctuations of the final atom numbers, i.e. 1100(300) atoms. The control of the position of the crossed dipole beam with respect to the standing light wave is crucial for the investigation of the dynamics of bosonic Josephson junctions. The relative shift determines the resulting shape of the effective double-well and its symmetry. In order to stabilize the position of the periodic potential, the relative phase of the two lattice laser beams is controlled with two acousto-optical modulators. The absolute position of the periodic potential maxima is deduced by coupling out 2% of the beam intensities and bringing them to interference under

an angle of $6(1)°$. This leads to an interference pattern with a periodicity of about 8 μm. A precision air slit with a width of $5(1)$ μm and a height of 3 mm is placed in the overlap region and is oriented parallel to the interference fringes. The light intensity transmitted through the slit, which directly depends on the relative phase between the two beams, is monitored with a photodiode. The signal of the photodiode is then locked to a given value using a standard proportional-integral loop amplifier. The achieved position stability is deduced by analyzing the position of the split-BEC images and gives an upper bound for the stability. We obtain a standard deviation of approximately 100 nm (limited by the pixel size of the camera system), which corresponds to a phase stability of less than $\pi/50$.

In order to initially prepare a given population imbalance, we use a controlled shift Δx of the crossed dipole trap beam which results in an asymmetric double-well potential, where more atoms are accumulated in the lower well. This shift is experimentally implemented with a piezo actuated mirror mount. The achievable population imbalances and the associated uncertainties are depicted in Fig. 2. For $\Delta x = 0$ the ramping up of the periodic potential into the condensate prepared in the harmonic potential leads to a symmetric population of both wells with vanishing population difference $z = (N_\mathrm{l} - N_\mathrm{r})/(N_\mathrm{l} + N_\mathrm{r}) = 0$ ($N_{\mathrm{l},\mathrm{r}}$ is the number of atoms in the left and right well, respectively). A shift of only $\Delta x = 500$ nm already introduces a population imbalance of $z_\mathrm{c} = 0.39$. As we will show in the last section, this corresponds to the critical imbalance for our experimental parameters which separates the regime of Josephson oscillation dynamics, i.e. $z < z_\mathrm{c}$ (indicated with gray shading in Fig. 2) and the self-trapping regime, i.e. $z > z_\mathrm{c}$. Clearly the experimental setup allows the preparation of both dynamical regimes. After the initial prep-
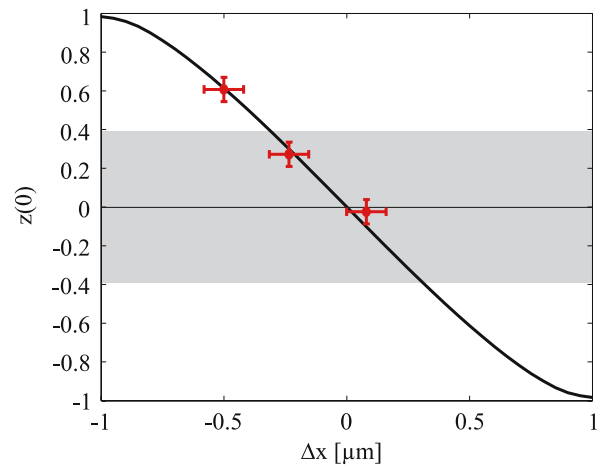

FIGURE 2 Preparation of the initial population imbalance. The *filled red circles* indicated the measured initial population imbalance corresponding to the two dynamical situations and the symmetric case. The condensate in the double-well potential is prepared by adiabatically ramping up the periodic potential. Since the symmetry of the effective double-well potential is given by the relative position Δx of the minimum of the crossed beam dipole trap and a maximum of the periodic potential the initial population can be adjusted by changing Δx. The graph reveals that the initial population imbalance can be created in the Josephson oscillation regime (indicated by the shading) and the self-trapping regime. The *solid line* is the theoretically predicted imbalance obtained by solving the non-polynomial Schrödinger equation numerically

aration of the BEC in an asymmetric double-well potential, i.e. $z \neq 0$ the dynamics are initiated by shifting the crossed dipole trap beam back to $\Delta x = 0$. The time scale of 7 ms is non-adiabatic with respect to the typical tunnelling time which is on the order of 50 ms. In order to understand the experimental observations quantitatively this finite response time has to be taken into account (see [6]).

The thorough calibration of all relevant parameters is the prerequisite for quantitative experiments. The harmonic confinement and the periodic potential are calibrated independently. The harmonic trapping frequencies are deduced from standard frequency measurements of dipolar oscillations. They are excited by reducing the intensities of the laser beams within less than 500 μs leading to dipolar oscillations with small amplitudes (few μm). These measurements lead to harmonic trapping frequencies of $\omega_x = 2\pi \times 78\,(1)$ Hz, $\omega_y \approx 2\pi \times 90\,(1)$ Hz and $\omega_z \approx 2\pi \times 66\,(1)$ Hz.

Since the tunnelling time is critically dependent on the thickness and height of the double-well barrier it is crucial to measure these parameters very accurately. As the width of the barrier is directly connected to the lattice spacing it can be measured in a straight forward way. A BEC of 2×10^4 atoms is loaded into a deep optical lattice ($V_0 \approx h \times 2$ kHz) superimposed on a harmonic trap $\omega_{x,y,z} = 2\pi \times (5, 120, 140)$ Hz leading to a periodic array of pancake condensates (see Fig. 3). For these parameters the influence of the shallow harmonic potential in the x-direction on the spacing of the potential is negligible, and thus the periodicity can be directly measured by analyzing the absorption image as shown in Fig. 3. From that measurement we deduce a lattice constant of $d_l = 5.18\,(9)$ μm.

The potential height of the periodic potential is directly connected to the barrier height. Due to the large well spacings the standard potential height calibration techniques do not work and thus we have developed a new method. The potential height is measured by observing the relative motion of two BECs in the double-well potential. This motion can be excited by switching off the harmonic confinement in the x-direction and ramping up the barrier height, i.e. the periodic potential height, by a factor of 5 within 2 ms. This procedure leads to a non-adiabatic increase of the double-well potential spacing $d_{dw} = 4.2$ μm to the lattice constant of the periodic potential $d_l = 5.18$ μm. The time scale of 2ms is chosen to reduce the collective excitations in the transverse direction but leads to very small oscillation amplitudes of approximately 400 nm (see Fig. 4). However, this change of the center of mass separation can still be measured with our optical imaging system
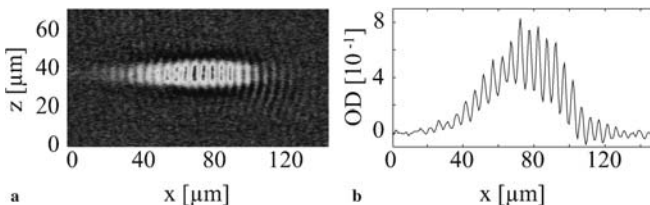

FIGURE 3 Calibration of the lattice spacing of the periodic potential. (**a**) The absorption image of the atomic cloud reveals the periodic arrangement of pancake BECs. (**b**) The density profile in x-direction directly shows the lattice spacing $d_l = 5.18\,(9)$ μm. From this measurement we can also deduce the optical resolution (sparrow-criterion) of our imaging system to be $3.2\,(2)$ μm
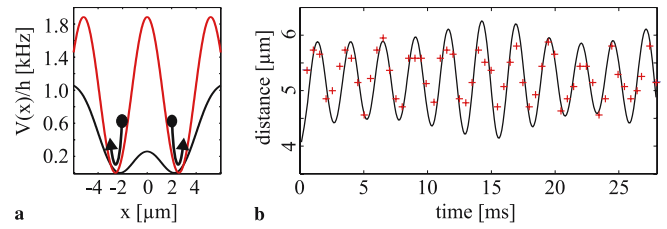

FIGURE 4 Calibration of the periodic potential height. (**a**) The BEC is first loaded into the effective double-well potential (*black solid line*). Subsequently the harmonic confinement in x-direction is switched off and the periodic potential height is increased to V_0. This leads to dipole oscillations in the individual wells as indicated. (**b**) The relative position of the two BECs in the optical lattice as a function of time after excitation reveal the potential height. The experimental data (*crosses*) are compared to the numerical simulation (*solid line*), which has only the lattice height as a free parameter. We find a potential height of $V_0 = h \times 412\,(20)$ Hz

which has an optical resolution of $3.2\,(2)$ μm as defined by the Sparrow-criterion. The experimental data are fitted with the result obtained from the integration of the non-polynomial Schrödinger equation [12] and a potential height of $V_0 = h \times 412\,(20)$ Hz is deduced. This corresponds to a barrier height of $V_b = h \times 263\,(20)$ Hz for the experimentally used harmonic confinement of $\omega_x = 2\pi \times 78$ Hz.

3 Josephson oscillations and self-trapping

In contrast to all hitherto realized Josephson junctions in superconductors and superfluids, in our experiment the interaction between the tunnelling particles plays a crucial role. This nonlinearity gives rise to new dynamical regimes. Josephson oscillations, i.e. oscillation of population imbalance and relative phase of the two condensates, are predicted [13–15], if the initial population imbalance of the two wells is below a critical value. The dynamics changes drastically for initial population differences above the threshold for macroscopic quantum self-trapping z_c [16–18] where large amplitude Josephson oscillations are inhibited and the phase difference increases in time.

The experimental protocol for investigating the dynamics is as follows: Rubidium atoms are precooled in a standard TOP trap, transferred into the crossed beam dipole trap and evaporatively cooled to degeneracy by lowering the light intensity. Finally the dipole laser beams and the optical lattice beams are ramped to the desired values. This sequence creates two weakly linked BECs inside an asymmetric double-well potential with well defined asymmetry and barrier height. The dynamics is initiated by shifting the crossed dipole beam realizing a symmetric double-well potential. After a given evolution time the potential barrier is suddenly ramped up and the dipole trap beam is switched off. This results in dipole oscillations of the atomic cloud around two neighboring minima of the periodic potential as used for the calibration of the periodic potential height (see Fig. 4). The atomic distribution is imaged at the time of maximum separation using absorption imaging techniques. This protocol has been used for the first demonstration of the transition between Josephson oscillations and macroscopic self-trapping in a single weak link [6]. In the following we shall show that the recent work by D. Ananikian and T. Bergeman [7] allows understanding of
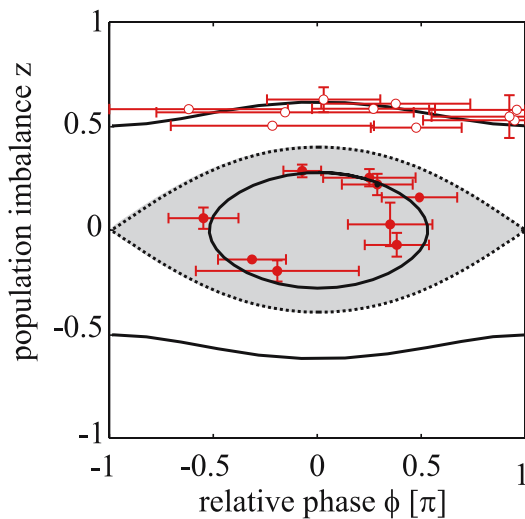
FIGURE 5 Comparison of the experimentally obtained phase plane trajectories to the predictions of the extended two-mode model (*solid lines*). The Josephson oscillation regime (*gray shaded region*) is characterized by closed trajectories (*filled circles*). The separatrix, which is represented by the dashed line, constitutes the transition to the self-trapped regime (*open circles*). It is important to note that there are no free parameters. Thus the improved two-mode tunnelling model explains our observation quantitatively

the experimental observation quantitatively with a relatively simple two-mode model.

The standard two-mode approximation assumes a weak link, i.e. the wave function overlap is negligible [18]. For our experimental parameters this is not strictly true. S. Giovanazzi et al. [19] have already included the leading term of the correction to the simple two-mode model but recently D. Ananikian and T. Bergeman managed to include all terms and present their improved two-mode model in [7]. They have derived differential equations for the basic two-mode parameters the population difference z and the relative phase between the two condensates. We will not elaborate on the theoretical description any further and refer the reader to reference [7] for details. Here, we report on the very good agreement of the prediction of this model with our experimental observation concerning the critical population imbalance distinguishing between the two different dynamical regimes. The simple constant tunnelling model predicts for our experimental parameters a critical population difference $z_c = 0.23$, but for this imbalance experimentally still Josephson oscillations are observed. From the experimental data we deduce $z_{exp} = 0.38(8)$ which is in very good agreement with the prediction of the improved two-mode model giving $z_c = 0.35$. This agreement is clearly revealed in Fig. 5 where the phase plane portrait predicted by the time varying tunnelling model (solid lines) and the experimental data (circles) are shown. It is important to note that there are no free parameters in this graph,

which is in contrast to the earlier reported phase–plane portrait [6], where the critical population difference was a free fit parameter.

Thus the observed dynamics can be understood in a simple two-mode model, but a time dependent tunnelling rate has to be taken into account. This finding is an important prerequisite for further investigations of more complex systems which are build up by Josephson junctions. One interesting direction is the controlled realization of many coupled weak links in two dimensions where the topology could have a big influence on the dynamics [20]. Also a very intriguing route is the investigation of the influence of the residual thermal cloud on the coherent dynamics [21]. Here, a completely new regime can be reached with the BEC system since the thermal cloud and thus the dissipation can be controlled.

REFERENCES

1 B.D. Josephson, Phys. Lett. **1**, 251 (1962)
2 P.L. Anderson, J.W. Rowell, Phys. Rev. Lett. **10**, 230 (1963)
3 S.V. Pereverzev, A. Loshak, S. Backhaus, J.C. Davis, R.E. Packard, Nature **388**, 449 (1997)
4 K. Sukhatme, Y. Mukharsky, T. Chui, D. Pearson, Nature **411**, 280 (2001)
5 F.S. Cataliotti, S. Burger, C. Fort, P. Maddaloni, F. Minardi, A. Trombettoni, A. Smerzi, M. Inguscio, Science **293**, 843 (2001)
6 M. Albiez, R. Gati, J. Fölling, S. Hunsmann, M. Cristiani, M.K. Oberthaler, Phys. Rev. Lett. **95**, 010402 (2005)
7 D. Ananikian, T. Bergeman, Phys. Rev. A, in press (available at http://xxx.lanl.gov/abs/cond-mat/0503220)
8 M.R. Andrews, C.G. Townsend, H.J. Miesner, D.S. Durfee, D.M. Kurn, W. Ketterle, Science **275**, 637 (1997)
9 T.G. Tiecke, M. Kemmann, Ch. Buggle, I. Schvarchuck, W. von Klitzing, J.T.M. Walraven, J. Opt. B **5**, 119 (2003)
10 Y. Shin, M. Saba, A. Schirotzek, T.A. Pasquini, A.E. Leanhardt, D.E. Pritchard, W. Ketterle, Phys. Rev. Lett. **92**, 150401 (2004)
11 J. Esteve, T. Schumm, J.B. Trebbia, I. Bouchoule, A. Aspect, C.I. Westbrook (available at http://xxx.lanl.gov/abs/physics/0503112, 2005)
12 L. Salasnich, A. Parola, L. Reatto, Phys. Rev. A **65**, 043614 (2002)
13 J. Javanainen, Phys. Rev. Lett. **57**, 3164 (1986)
14 M.W. Jack, M.J. Collett, D.F. Walls, Phys. Rev. A **54**, R4625 (1996)
15 I. Zapata, F. Sols, A.J. Leggett, Phys. Rev. A **57**, R28 (1998)
16 G.J. Milburn, J. Corney, E.M. Wright, D.F. Walls, Phys. Rev. A **55**, 4318 (1997)
17 A. Smerzi, S. Fantoni, S. Giovanazzi, S.R. Shenoy, Phys. Rev. Lett. **79**, 4950 (1997)
18 S. Raghavan, A. Smerzi, S. Fantoni, S.R. Shenoy, Phys. Rev. A **59**, 620 (1999)
19 S. Giovanazzi, A. Smerzi, S. Fantoni, Phys. Rev. Lett. **84**, 4521 (2000)
20 private communication with Pasquale Sodano and Andrea Trombettoni
21 L. Pitaevskii, S. Stringari, Phys. Rev. Lett. **87**, 180402 (2001)